Available online at www.sciencedirect.com
ScienceDirect
Finite Elements in Analysis and Design 44 (2008) 472–482
FINITE ELEMENTS IN ANALYSIS AND DESIGN
www.elsevier.com/locate/finel

A stabilized mixed formulation for finite strain deformation for low-order tetrahedral solid elements

R. Cisloiu[b,*], M. Lovell[a], J. Wang[b]

[a]*Department of Mechanical and Industrial Engineering, University of Pittsburgh, Pittsburgh, PA 15261, USA*
[b]*ANSYS, Inc., 275 Technology Drive, Canonsburg, PA 15317, USA*

Received 26 February 2007; received in revised form 8 November 2007; accepted 5 January 2008
Available online 13 February 2008

Abstract

A stabilized mixed finite element formulation for four-noded tetrahedral elements is introduced for robustly solving small and large deformation problems. The uniqueness of the formulation lies within the fact that it is general in that it can be applied to any type of material model without requiring specialized geometric or material parameters. To overcome the problem of volumetric locking, a mixed element formulation that utilizes linear displacement and pressure fields was implemented. The stabilization is provided by enhancing the rate of deformation tensor with a term derived using a bubble function approach. The element was implemented through a user-programmable element of the commercial finite element software ANSYS. Using the ANSYS platform, the performance of the element was evaluated by comparing the predicted results with those obtained using mixed quadratic tetrahedral elements and hexahedral elements with a B-bar formulation. Based on the quality of the results, the new element formulation shows significant potential for use in simulating complex engineering processes.

Keywords: Bubble function; Tetrahedral finite element; Finite strain deformation; Stabilized finite element method; Incompressibility

1. Introduction

In the engineering community, greater efficiency in the design process can be attained by creating seamless interfaces between CAD geometries and finite element models. Given the fact that tetrahedral meshing of CAD geometries is robust and fast, the development of higher quality tetrahedral elements has become an important need in the finite element analysis community. This need has been accentuated by the fact that the finite element industry has introduced automated rezoning features that utilize tetrahedral elements. These linear elements are very attractive because they are simple and less sensitive to distortion which makes them suitable for large deformation analyses. As noted in the literature [1], there does not exist a single tetrahedral element that performs well across a broad class of engineering problems. This is primarily due to the fact that the linear displacement based formulations of tetrahedral elements exhibit severe volumetric locking when used with incompressible materials and show stiff behavior in bending dominant problems. To eliminate these problems, several different techniques have evolved in the literature. The most commonly used technique employs mixed displacement/pressure elements in which the pressure field is considered an independent variable. When such mixed methods are utilized, the resulting elements possess instabilities in the pressure field. These instabilities occur because the mixed displacement–pressure formulations use an equal order interpolation that does not pass the Babuška–Brezzi (BB) condition [2].

Over the last several years, researchers have employed specialized stabilization techniques to circumvent the strict BB condition while using the same order of interpolation functions. This has been especially true in the field of incompressible fluid dynamics where successful approaches have been achieved that can be extended to the solid mechanics domain. Among the works that focused on stabilizing solid tetrahedrons, formulations were developed to address problems related to small deformations using incompressible elastic materials [3–5], plastic materials [6–8], and large deformations in the context of hyperelastic materials [9,10]. All of the formulations can be

* Corresponding author. Tel.: +1 724 514 2947; fax: +1 724 514 3118.
E-mail address: roxana.cisloiu@ansys.com (R. Cisloiu).

0168-874X/$ - see front matter © 2008 Elsevier B.V. All rights reserved.
doi:10.1016/j.finel.2008.01.003

generally classified into the following categories: (1) stabilization by employing finite element approximations enriched with so-called "bubble" functions [11], (2) stabilization by adding mesh-dependent perturbation terms [9], (3) mixed-enhanced strain stabilization [10], (4) orthogonal sub-grid scale methods [3,4,6], (5) finite increment calculus (FIC) methods [5], and (6) average nodal pressures or nodal deformation gradient techniques [12].

The first effort to stabilize lower-order elements for the incompressible Navier-Stokes problem was the "MINI" element introduced by Arnold et al. [11]. This is an attractive linear triangular element with a displacement interpolation enhanced with a cubic bubble function. The element satisfies the strict BB condition and has few degrees of freedom and no mesh and material dependent parameters. Two shortcomings of the element are related to the persistence of some small pressure oscillations and the influence of the bubble mode on the inertial terms in transient problems. Another set of stabilization techniques have been based on modifications to the discrete equation of volumetric constraints rather than interpolation functions. This method was first introduced by Brezzi and Pitkäranta [13] for stabilizing finite element approximations to the Stokes problem. Other alternatives were later developed for incompressible elasticity and finite elasticity. Even though the general method provides a stabilized pressure field, the addition of a non-zero diagonal terms does not have a strong theoretical foundation. In this regard, the formulation requires the choice of a parameter that depends on the material shear modulus and element edge length which makes it prone to instabilities in large deformation problems.

A mixed-enhanced strain stabilization technique was later introduced by Zienkiewicz and Taylor [14] and implemented by Taylor [10] for low-order tetrahedral elements experiencing both small and finite deformations. Taylor's implementation used a three-field approximation that incorporated continuous displacement and pressure, discontinuous volume changes, and an enhanced strain formulation. The enhanced strains were added to the traditional strains to provide the necessary stabilization for nearly incompressible conditions. The method was formulated for hyperelastic materials for which a strain energy density function existed. This formulation, however, cannot be applied to materials where a strain energy function cannot be defined.

A sub-grid scale stabilization approach (OSGS) was first proposed by Hughes [15] and recently modified by Codina [16] for incompressible fluid dynamics. Chiumenti further extended the method to solid mechanics in the context of incompressible elasticity [4] and J2 plasticity [5]. The underlying theory of the method involves decomposing the continuous fields into coarse and fine components that correspond to the different length scales. The fine or sub-grid displacement is found on the space orthogonal to the finite element space which allows a stabilization term to appear in the incompressibility constraint equation that is dependent on the sub-grid displacements. The method was successfully applied in fluid dynamics since it circumvents the BB condition and yields results free of volumetric locking and pressure oscillations. Some of its limitations include the dependence on material and geometry parameters, and its expensive computational cost due to the introduction of another continuous variable, the projection of the pressure gradient, which increases the number of active degrees of freedom from 16 to 28. The application of this method for large deformation behavior is less general because it is formulated in the context of J2 plasticity as a function of shear modulus and element length.

The most recent approach in stabilizing the mixed u/p elements is the FIC method. Even though the approach is completely different from the OSGS method, it yields the same formulation. The basis of the FIC formulation hinges upon satisfying the standard equations of equilibrium in a domain of finite size. In the FIC, the differential equation terms are expressed using a Taylor series expansion where the higher-order terms are retained. The resulting equations are enhanced with some additional terms, which introduce the necessary stability to overcome volumetric locking. This method was first developed by Onate for advective–diffusive and fluid flow problems [17] and was later applied to incompressible solids [5]. The FIC method has a strong theoretical basis and yields accurate results without introducing pressure oscillations. Its extension to finite deformations, however, can be difficult because the stabilization parameters depend on materials and characteristic lengths which are not well defined. Similar to the OSGS method, the FIC method is computationally expensive due to the introduction of a new continuous field variable, the projected pressure gradient.

Evaluating the methods available for stabilizing tetrahedral elements, we can conclude that the pressure stabilization, OSGS and FIC methods yield similar stabilization terms in the constraint equation. The only differences in these methods are the projected pressure gradient terms which are not significant in static analyses. In addition, several authors have shown the equivalence between the bubble and stabilized methods. Hughes [15], for example, established a relationship between the 'bubble function', stabilized methods and sub-grid scale methods. Pierre [18] also showed that by eliminating the cubic bubble using static condensation, the stabilized methods are recovered. A key feature of most of the stabilization methods in the literature is that they make use of material and geometry dependent parameters which can impose serious limitations in a general purpose finite element code. At present, there is no general formulation that is applicable to both a general finite strain deformation and a large class of nonlinear materials.

2. Theoretical formulation

2.1. General aspects

In this paper, an enhanced deformation rate formulation that is based on the approach of Taylor [10] will be developed for lower-order tetrahedral solid elements. The elements will be developed to solve problems involving small deformations, large deformations and large rotations. The novelty of the formulation lies within the fact that no specialized geometric or material model parameters are required. Since the proposed formulation

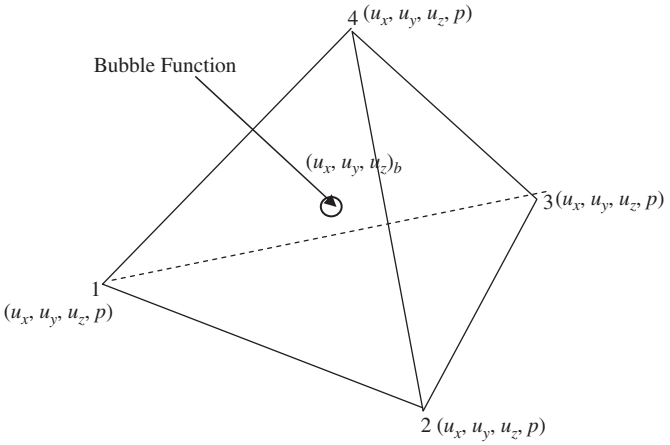

Fig. 1. Tetrahedral element.

is applicable to general finite strain deformation, it has to take into consideration the following [19]: (1) the geometry changes during deformation, (2) the fact that the strain is no longer infinitesimal so that large strain definitions must be employed, (3) the Cauchy stress cannot be updated by simply adding its increment due to straining of the material (it has to take into account the rigid body rotations), (4) the nonlinear behavior has to be based on an incremental approach. Therefore an updated Lagrangian procedure was employed to solve for the geometric nonlinearities. According to this procedure, all the quantities were evaluated at time $t+\Delta t$ in terms of the solved variables at time t.

As shown in Fig. 1, the proposed element has a node in each corner (with displacement and pressure as external degrees of freedom) and a node located in the barycenter [18] that has enhanced deformation parameters as internal degrees of freedom. The enhanced deformation parameters will be derived from a bubble function.

2.2. Governing equations

Following the updated Lagrangian approach used by Sussman and Bathe [19] in the development of the mixed u/p formulation, the finite element equations of motion will be derived from the principle of virtual work using the last converged configuration as the reference configuration. The basic equilibrium equation using the principle of virtual work can be expressed as [20,21]

$$\int_V \sigma_{ij}\delta e_{ij}\,\mathrm{d}V = \int_V b_i\delta u_i\,\mathrm{d}V + \int_S f_i\delta u_i\,\mathrm{d}S, \tag{1}$$

$$\delta e_{ij} = \frac{1}{2}\left(\frac{\partial\delta u_i}{\partial x_j} + \frac{\partial\delta u_j}{\partial x_i}\right),$$

where δe_{ij} is the virtual deformation tensor computed in current configuration, $\sigma_{ij}$are the components of Cauchy stress, δu_i are the components of the virtual displacement field, f_i are the components of the externally applied surface tractions on the surface S bounding the volume V, and b_i are the components of body forces per unit volume.

The mixed displacement–pressure formulation requires that the hydrostatic pressures be interpolated at the element level. Therefore, the Cauchy stress is modified as

$$\begin{aligned}\overline{\sigma_{ij}} &= \sigma_{ij}^{\mathrm{dev}} + \delta_{ij}\overline{P} = \sigma_{ij} - \delta_{ij}P + \delta_{ij}\overline{P}\\ &= \sigma_{ij} + \delta_{ij}(\overline{P} - P),\end{aligned} \tag{2}$$

where $\sigma_{ij}^{\mathrm{dev}}$ is the deviatoric part of the Cauchy stress, P is the pressure derived from Cauchy stress, and $\overline{P}$ is the interpolated pressure.

In addition to the pressures, the volumetric part of the deformation tensor was also interpolated at the element level, modifying the deformation tensor as

$$\overline{e}_{ij} = e_{ij}^{\mathrm{dev}} + \tfrac{1}{3}\delta_{ij}\overline{e}_v = e_{ij} - \tfrac{1}{3}\delta_{ij}(e_v - \overline{e}_v), \tag{3}$$

where $\overline{e}_{ij}$ is the modified deformation tensor, and e_{ij}^{dev} and $\overline{e}_{\mathrm{v}}$ are its deviatoric and interpolated volumetric parts, respectively.

If a three-field form of the principle of virtual work is used, two additional constraint equations must be enforced in the principle of virtual work by means of two Lagrange multipliers, $\delta\overline{P}$ and $\delta\overline{e}_{\mathrm{v}}$. The augmented internal virtual work will therefore have the form

$$\begin{aligned}\delta W_{\mathrm{int}} = &\int_V \overline{\sigma}_{ij}\delta e_{ij}\,\mathrm{d}V + \int_V (P-\overline{P})\delta\overline{e}_{\mathrm{v}}\,\mathrm{d}V\\ &+ \int_V (e_{\mathrm{v}} - \overline{e}_{\mathrm{v}})\delta\overline{P}\,\mathrm{d}V.\end{aligned} \tag{4}$$

For efficiency and simplification of implementation, the above formulation can be reduced to a mixed displacement pressure form by taking out the constraint $e_{\mathrm{v}} - \overline{e}_{\mathrm{v}} = 0$ that corresponds to the volumetric deformation variable:

$$\delta W_{\mathrm{int}} = \int_V \overline{\sigma}_{ij}\delta e_{ij}\,\mathrm{d}V + \int_V (P-\overline{P})\delta\overline{e}_{\mathrm{v}}\,\mathrm{d}V. \tag{5}$$

Expressing the interpolated pressure in terms of interpolated volumetric deformation tensor components we find

$$\begin{aligned}\delta\overline{P} &= \tfrac{1}{3}\delta_{ij}\overline{\sigma}_{ij} = \tfrac{1}{3}\delta_{ij}C_{ijkl}\delta e_{kl} = \tfrac{1}{3}\delta_{ij}C_{ijkl}\left(\delta e_{kl}^{\mathrm{dev}} + \frac{1}{3}\delta_{kl}\delta\overline{e}_{\mathrm{v}}\right)\\ &= \frac{1}{3}\delta_{ij}C_{ijkl}\delta e_{kl}^{\mathrm{dev}} + K\delta\overline{e}_{\mathrm{v}},\end{aligned} \tag{6}$$

where $K = \frac{1}{9}\delta_{ij}C_{ijkl}\delta_{kl}$ is the instantaneous bulk modulus.

Modifying the Lagrange multiplier for the pressure constraint equation it is determined

$$\begin{aligned}\delta\overline{e}_{\mathrm{v}} = &\frac{\delta\overline{P}}{K} - \frac{1}{3K}\delta_{ij}C_{ijkl}\delta e_{kl}^{\mathrm{dev}} = \frac{\delta\overline{P}}{K}\\ &- \frac{1}{3K}\delta_{ij}C_{ijkl}\delta e_{kl} + \delta e_{\mathrm{v}}.\end{aligned} \tag{7}$$

If Eq. (5) is differentiated with respect to time and only the linear differential terms are retained, the following virtual work equation in rate form is obtained:

$$\begin{aligned}\delta\dot{W}_{\mathrm{int}} = &\int_V \frac{D\overline{\sigma}_{ij}}{Dt}\delta e_{ij}\,\mathrm{d}V + \int_V \frac{D\delta e_{ij}}{Dt}\overline{\sigma}_{ij}\,\mathrm{d}V\\ &+ \int_V \frac{D}{Dt}(P-\overline{P})\delta\overline{e}_{\mathrm{v}}\,\mathrm{d}V.\end{aligned} \tag{8}$$

As shown in Lee [20] for the limiting case,

$$\lim_{\Delta t\to 0}\left\{\frac{\Delta\overline{\sigma}_{ij}}{\Delta t};\frac{\Delta e_{ij}}{\Delta t};\frac{\Delta\overline{e}_{\mathrm{v}}}{\Delta t};\frac{\Delta u_{i,j}}{\Delta t};\frac{\Delta u_i}{\Delta t};\frac{\Delta f_i}{\Delta t}\right\} = \left\{\dot{\overline{\sigma}}_{ij};D_{ij};\overline{D}_v;v_{i,j};v_i;\dot{f}_i\right\}, \tag{9}$$

the virtual work equation in incremental form is exactly the same as the virtual work equation in rate form

$$D\delta W_{\mathrm{int}} = \int_V D\overline{\sigma}_{ij}\delta D_{ij}\,\mathrm{d}V + \int_V \overline{\sigma}_{ij}\delta D_{ij}\,\mathrm{d}V + \int_V (DP - D\overline{P})\delta\overline{D}_{\mathrm{v}}\,\mathrm{d}V, \tag{10}$$

where D_{ij} are the components of the deformation rate tensor defined as the symmetric gradient of the velocity tensor:

$$D_{ij} = \frac{1}{2}\left(\frac{\partial v_i}{\partial x_j} + \frac{\partial v_j}{\partial x_i}\right). \tag{11}$$

A linearized system of equations can then be established in increments of the unknown variables:

$$D\delta W_{\mathrm{int}} = \int_V D\overline{\sigma}_{ij}\delta D_{ij}\,\mathrm{d}V + \int_V \overline{\sigma_{ij}}\delta D_{ij}\,\mathrm{d}V + \int_V \left(\frac{1}{3}\delta_{ij}C_{ijkl}D_{kl}\right)\delta\overline{D}_{\mathrm{v}}\,\mathrm{d}V - \int_V \delta\overline{D}_{\mathrm{v}}D\overline{P}\,\mathrm{d}V. \tag{12}$$

The increment of Cauchy stress is divided into two different parts: one due to the rigid body motion only and one associated with the rate form of the stress–strain law. Since $\overline{\sigma}$ and σ differ only in the hydrostatic part, it can be written that

$$\dot{\overline{\sigma}}_{ij} = C_{ijkl}D_{kl} + \overline{\sigma}_{ik}\dot{\omega}_{jk} + \overline{\sigma}_{jk}\dot{\omega}_{ik}, \tag{13}$$

where $C_{ijkl}D_{kl}$ is the Jaumann stress rate associated with the rate form of the stress–strain law, C_{ijkl} are the components of material constitutive tensor, D_{kl} are the components of the deformation rate tensor, ω_{ij} are the components of the rotation tensor, and $\dot{\omega}_{ij}$ are the components of the spin tensor. An integration process is then required to evaluate the Cauchy stresses to make it suitable for an analysis of path-dependent materials [22].

Differentiating (7) and introducing (13) into the incremental expression of internal virtual work (12), we express the linearized internal virtual work by

$$D\delta W_{\mathrm{int}} = \int_V \left(\delta D_{ij}C_{ijkl}D_{kl}\,\mathrm{d}V - DP\frac{\delta_{ij}}{3K}C_{ijkl}\delta D_{kl}\right)\mathrm{d}V + \int_V DP\frac{\delta D\overline{P}}{K}\,\mathrm{d}V - \int_V D\overline{P}\frac{\delta D\overline{P}}{K}\,\mathrm{d}V + \int_V D\overline{P}\frac{\delta_{ij}}{3K}C_{ijkl}\delta D_{kl}\,\mathrm{d}V + \int_V [\delta D_{ij}(\overline{\sigma}_{ik}D\omega_{jk} + \overline{\sigma}_{jk}D\omega_{ik}) + \overline{\sigma}_{ij}\delta D_{ij}]\,\mathrm{d}V. \tag{14}$$

The last integral represents the nonlinear geometric term whose final expression is given in [23] by

$$\overline{\sigma}_{ik}D\omega_{jk}\delta D_{ij} + \overline{\sigma}_{jk}D\omega_{ik}\delta D_{ij} + \overline{\sigma}_{ij}\delta D_{ij} = \overline{\sigma}_{ij}\left(\frac{\partial Du_k}{\partial x_i}\frac{\partial\delta Du_k}{\partial x_j} - 2\delta D_{ik}D_{kj}\right). \tag{15}$$

Introducing (15) in (14), we obtain the following formulation that was used for the user-programmable element that interfaced with ANSYS:

$$D\delta W_{\mathrm{int}} = \int_V \left(\delta D_{ij}C_{ijkl}D_{kl} - \frac{1}{9K}\delta D_{ij}C^{\mathrm{T}}_{ijmn}\delta_{mn}\delta_{op}C_{opkl}D_{kl}\right)\mathrm{d}V + \int_V \overline{\sigma}_{ij}\left(\frac{\partial Du_k}{\partial x_j}\frac{\partial\delta Du_k}{\partial x_i} - 2\delta D_{ik}D_{jk}\right)\mathrm{d}V - \int_V D\overline{P}\frac{1}{K}\delta D\overline{P}\,\mathrm{d}V + \int_V \frac{1}{3K}\delta_{ij}C_{ijkl}D_{kl}\delta D\overline{P}\,\mathrm{d}V + \int_V D\overline{P}\frac{1}{3K}\delta_{ij}C_{ijkl}\delta D_{kl}\,\mathrm{d}V. \tag{16}$$

2.3. Enhanced deformation gradient

Our proposed stabilization technique is based on enhancing the deformation mode. The key aspect of this type of formulation is to modify the deformation gradient with an independent field which is considered discontinuous across the element. Through this modification, the element will be free from locking in the incompressibility limit [24]. The improved representation of the deformation gradient increment then takes the form

$$\Delta F^{\mathrm{enh}}_{ij} = \Delta F_{ij} + \Delta\overline{F}_{ij} \tag{17}$$

which can also be written in terms of incremental displacements as

$$\Delta F^{\mathrm{enh}}_{ij} = \frac{\partial^{t+\Delta t}x_i}{\partial^t x_j} = \frac{\partial({}^t x_i + Du_i)}{\partial^t x_j} + \Delta\overline{F}_{ij}. \tag{18}$$

The enhanced part of the deformation gradient increment, $\Delta\overline{F}_{ij}$, is computed using the independent internal incremental displacements as

$$\Delta F^{\mathrm{enh}}_{ij} = \delta_{ij} + \frac{\partial Du_i}{\partial^t x_j} + \frac{\partial Du^{(b)}_i}{\partial^t x_j}, \tag{19}$$

where Du_i and $Dui^{(b)}$ are, respectively, the external and internal increments in displacements.

The total enhanced deformation gradient from the initial configuration is calculated as

$${}^{t+\Delta t}_{0}F^{\mathrm{enh}} = {}^{t+\Delta t}_{t}\Delta F^{\mathrm{enh}}\cdot{}^{t}_{0}F^{\mathrm{enh}}. \tag{20}$$

The volume has to be modified consistently as

$$\mathrm{d}V^{t+\Delta t} = |{}^{t+\Delta t}_{0}F^{\mathrm{enh}}|\,\mathrm{d}V^0 = |\Delta F^{\mathrm{enh}}|\cdot\mathrm{d}V^t. \tag{21}$$

As addressed in the following section, the modification of the deformation gradient and of the current volume implies that the rate of deformation tensor needs to be enhanced.

2.4. Matrix formulation

For the isoparametric tetrahedral element, the interpolation of the reference geometry, and of the rates of the degrees of freedom can be written in terms of parametric coordinates, ξ, and the corresponding nodal values:

$$X(\xi) = \sum_{\alpha=1}^{4} N^{\alpha}(\xi) X^{\alpha} = N \cdot X,$$

$$v(\xi) = \frac{Du(\xi)}{Dt} = \frac{1}{Dt} \sum_{\alpha=1}^{4} N^{\alpha}(\xi) Du^{\alpha} = N \cdot v,$$

$$D\overline{P}(\xi) = \sum_{\alpha=1}^{4} N^{\alpha}(\xi) \overline{P}^{\alpha} = N \cdot D\overline{P}. \tag{22}$$

The shape functions for the linear tetrahedron are simply the parametric coordinates. Each of them is unity for one node and zero at the others and varies linearly everywhere

$$N_1 = \xi_1,$$

$$N_2 = \xi_2,$$

$$N_3 = \xi_3,$$

$$N_4 = \xi_4 = 1 - \xi_1 - \xi_2 - \xi_3. \tag{23}$$

Usually the deformation rate tensor components are computed using the symmetric gradient of the shape functions as

$$D(\xi) = B(\xi) \cdot v = B(\xi) \cdot \frac{Du}{Dt}^{\alpha}. \tag{24}$$

In our proposed formulation the deformation rate tensor is enhanced with a stabilizing term derived from the bubble function. The matrix B, which relates the deformation rate to the nodal velocities, is then enlarged with three additional columns that are obtained by taking the symmetric gradient of the bubble function. Therefore, the enhanced deformation rate matrix has the form

$$B^{\mathrm{enh}} = \begin{bmatrix} \frac{\partial N_1}{\partial x_1} & 0 & 0 & & \frac{\partial N_b}{\partial x_1} & 0 & 0 \\ 0 & \frac{\partial N_1}{\partial x_2} & 0 & & 0 & \frac{\partial N_b}{\partial x_2} & 0 \\ 0 & 0 & \frac{\partial N_1}{\partial x_3} & & 0 & 0 & \frac{\partial N_b}{\partial x_3} \\ \frac{\partial N_1}{\partial x_2} & \frac{\partial N_1}{\partial x_1} & 0 & & \frac{\partial N_b}{\partial x_2} & \frac{\partial N_b}{\partial x_1} & 0 \\ 0 & \frac{\partial N_1}{\partial x_3} & \frac{\partial N_1}{\partial x_2} & & 0 & \frac{\partial N_b}{\partial x_3} & \frac{\partial N_b}{\partial x_2} \\ \frac{\partial N_1}{\partial x_3} & 0 & \frac{\partial N_1}{\partial x_1} & \alpha = 1,4 & \frac{\partial N_b}{\partial x_3} & 0 & \frac{\partial N_b}{\partial x_1} \end{bmatrix}. \tag{25}$$

A cubic bubble function was selected and it was defined as [18]

$$N_{\mathrm{b}} = (N+1)^{(N+1)} \prod_{i=1}^{N+1} \xi_i,$$

where $N = 2$ for triangle and $N = 3$ for tetrahedral elements.

Each of the integrals from the linearized expression of the internal virtual work yields the specific stiffness term associated with the corresponding variable as

1. Constitutive stiffness matrix:

$$K_{uu}^{\mathrm{enh,c}} = \int_V B^{\mathrm{enh}^{\mathrm{T}}} \left(C - \frac{1}{9K} C^{\mathrm{T}} \cdot I \cdot I \cdot C \right) B^{\mathrm{enh}} \, \mathrm{d}V. \tag{26}$$

2. Displacement pressure stiffness matrices:

$$K_{up}^{\mathrm{enh}} = (K_{pu}^{\mathrm{enh}})^{\mathrm{T}} = \int_V \frac{1}{3K^t} B^{\mathrm{enh}^{\mathrm{T}}} C^{\mathrm{T}} \cdot I \cdot N \, \mathrm{d}V. \tag{27}$$

3. Pressure stiffness matrix:

$$K_{pp} = \int_V -\frac{1}{K} N^{\mathrm{T}} \cdot N \, \mathrm{d}V. \tag{28}$$

In (26)–(28), the Voigt matrix notation was used such that each second rank tensor was written as a vector and each fourth rank tensor was written as a matrix.

4. Geometric stiffness matrix
When large deformations are expected the geometric stiffness matrix is added to the constitutive stiffness matrix. This is given by

$$K_{uu}^{\mathrm{enh},g} = \int_V [N_{,i}^{\mathrm{enh}}][\sigma_{ij}][N_{,j}^{\mathrm{enh}}] \, \mathrm{d}V - \int_V [B_{ki}^{\mathrm{T,enh}}][\sigma_{ij}][B_{kj}^{\mathrm{enh}}] \, \mathrm{d}V, \tag{29}$$

where $[N_{,i}^{\mathrm{enh}}]$ is the enhanced gradient of shape functions matrix. This matrix is formed by taking the derivatives of the shape and bubble functions with respect to the current configuration. The stress matrix is then written as

$$[\overline{\sigma}_{ij}] = \begin{bmatrix} \overline{\sigma}_{11} & \overline{\sigma}_{12} & \overline{\sigma}_{13} & 0 & 0 & 0 & 0 & 0 & 0 \\ \overline{\sigma}_{21} & \overline{\sigma}_{22} & \overline{\sigma}_{23} & 0 & 0 & 0 & 0 & 0 & 0 \\ \overline{\sigma}_{31} & \overline{\sigma}_{32} & \overline{\sigma}_{33} & 0 & 0 & 0 & 0 & 0 & 0 \\ 0 & 0 & 0 & \overline{\sigma}_{11} & \overline{\sigma}_{12} & \overline{\sigma}_{13} & 0 & 0 & 0 \\ 0 & 0 & 0 & \overline{\sigma}_{21} & \overline{\sigma}_{22} & \overline{\sigma}_{23} & 0 & 0 & 0 \\ 0 & 0 & 0 & \overline{\sigma}_{31} & \overline{\sigma}_{31} & \overline{\sigma}_{33} & 0 & 0 & 0 \\ 0 & 0 & 0 & 0 & 0 & 0 & \overline{\sigma}_{11} & \overline{\sigma}_{12} & \overline{\sigma}_{13} \\ 0 & 0 & 0 & 0 & 0 & 0 & \overline{\sigma}_{21} & \overline{\sigma}_{22} & \overline{\sigma}_{23} \\ 0 & 0 & 0 & 0 & 0 & 0 & \overline{\sigma}_{31} & \overline{\sigma}_{32} & \overline{\sigma}_{33} \end{bmatrix} \tag{30}$$

and $[B_{kj}^{\mathrm{enh}}]$ is the enhanced symmetric gradient of the shape functions with respect to the current configuration.

2.5. Element implementation aspects

The basic equations employed in this formulation were the Jaumann stress rate equation (13) and the incremental virtual work equation (16). All of the terms in these equations were evaluated at time $t + \Delta t$ in terms of the solved variables at time t. By doing this, the element matrices and load vectors can be derived and arranged as a linear system of equations as

$$\begin{bmatrix} K_{uu}^{\mathrm{enh}} & K_{up}^{\mathrm{enh}} \\ K_{pu}^{\mathrm{enh}} & K_{pp} \end{bmatrix} \begin{bmatrix} Du^{\mathrm{enh}} \\ D\overline{P} \end{bmatrix} = \begin{bmatrix} F^{\mathrm{ext}} - F_u^{\mathrm{enh}} \\ 0 - F_p \end{bmatrix}, \tag{31}$$

where $K_{uu}^{\text{enh}} = K_{uu}^{\text{enh,c}} + K_{uu}^{\text{enh,g}}$ is a square matrix of size 15×15, Du^{enh} is the enhanced vector of incremental displacements of size 15, F_u^{enh} is the enhanced internal force resulting from the equilibrium equation computed from

$$F_u^{\text{enh}} = \int_V (B^{\text{enh}})^{\text{T}} \cdot \overline{\sigma}\, \mathrm{d}V, \tag{32}$$

F_p is the residual of the constraint equation due to mixed u/p formulation calculated as

$$F_p = \int_V (DP - D\overline{P})\delta D\overline{P} \frac{1}{K}\, \mathrm{d}V, \tag{33}$$

where

$$DP = P^{t+\Delta t} - P^t = \tfrac{1}{3}(\sigma_1^{t+\Delta t} + \sigma_2^{t+\Delta t} + \sigma_3^{t+\Delta t}) - \tfrac{1}{3}(\sigma_1^t + \sigma_2^t + \sigma_3^t). \tag{34}$$

The solution of the system in (31) was performed in two steps. In the first step the internal parameters were eliminated at the element level by static condensation. In the second step, the Newton–Raphson iteration technique was utilized to solve the global system. Before the static condensation procedure, the size of the final stiffness matrix and of the displacement and force vectors was 19. After the static condensation procedure, a reduced stiffness matrix and load vectors were obtained such that the final size of the stiffness matrix, load vector and the vector of the external degrees of freedom was 16.

Generally, in a history-dependent problem the strain and stress (which are history-dependent variables) have to be integrated over the increment of each iteration. In our formulation the strain is defined as the integral of the deformation rate. The integration process has to take into account the fact that the principal axes of strain and stress rotate during the deformation. For this reason, the strain and stress at the beginning of the increment must be rotated with the amount of rigid body rotation that occurs during that increment. This is done using the Hughes–Winget [25] algorithm:

$$\sigma_{t+\Delta t} = \Delta R \cdot \sigma_t \cdot \Delta R^{\text{T}} + D\sigma, \tag{35}$$

where ΔR is the rotation matrix computed from the polar decomposition of the deformation gradient increment at the midpoint configuration, and $D\sigma$ is the material response part of the stress increment (Jaumann stress rate) which in component form is

$$D\sigma_{ij} = C_{ijkl} D_{kl} \tag{36}$$

and the deformation rate, D, is defined by the central difference formula as

$$D = sym\left(\frac{\partial v}{\partial x_{t+\Delta t/2}}\right), \tag{37}$$

where

$$x_{t+\Delta t/2} = \tfrac{1}{2}(x_t + x_{t+\Delta t}). \tag{38}$$

3. Numerical examples

Using the formulation outlined in Section 2, a user-programmable element was implemented into the commercial finite element code ANSYS with three different element options. These options were developed to demonstrate what improvement the proposed formulation offered over existing pure displacement and mixed u/p formulations. The three specific options coded included: (1) a mixed u/p enhanced stabilization with a cubic bubble function, (2) a mixed u/p without stabilization and (3) a pure displacement. After the numerical algorithms were linked to ANSYS, their accuracy was verified by solving known benchmark problems for which results were available [21].

3.1. Uniaxial tension test

As a means of verifying the new element formulation, a homogeneous deformation patch test was carried to determine the new element's ability to sustain constant strain states at large deformations. As shown in Fig. 2, the finite element model for

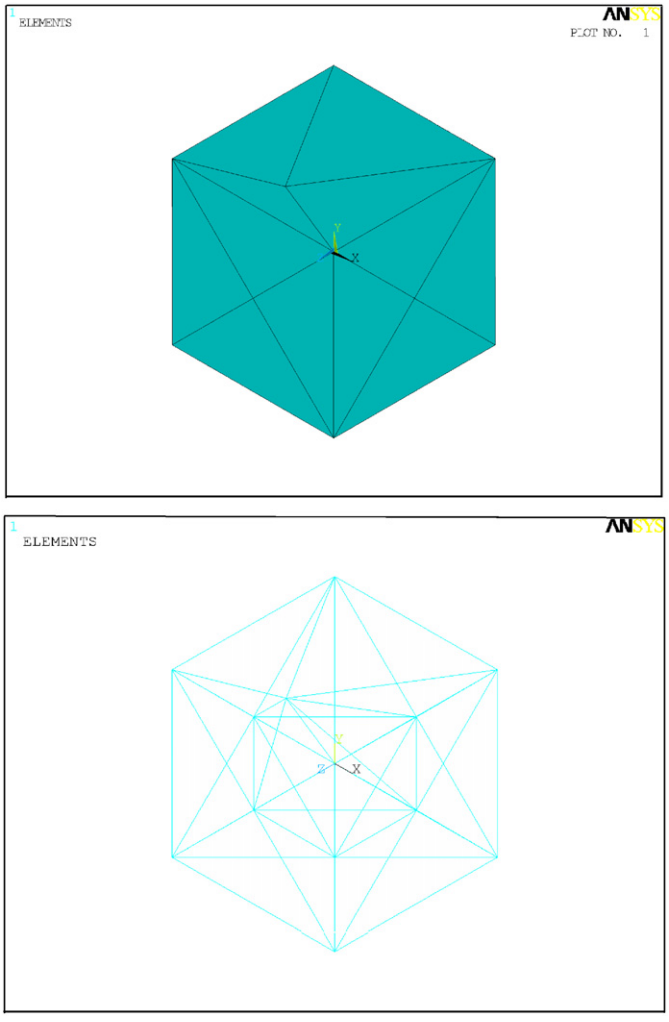

Fig. 2. Homogeneous deformation test: mesh.

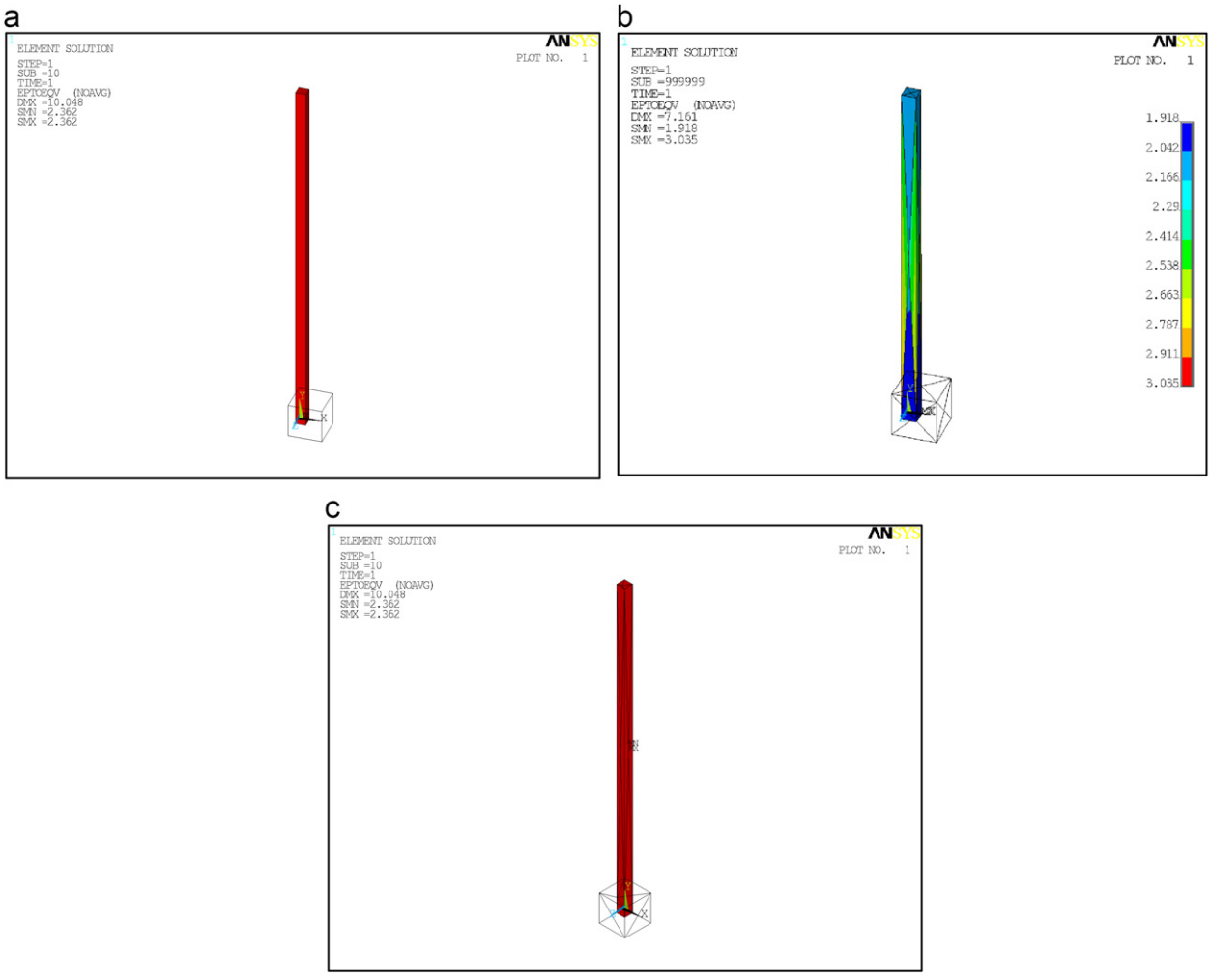

Fig. 3. Homogeneous deformation test: equivalent strain. (a) Mixed u/p hexahedral, (b) constant pressure 10 node tetrahedral, (c) stabilized mixed u/p four-node tetrahedral.

the test consisted of a cube with a side length of one that was made up of 29 tetrahedral elements. In the model, three adjacent faces of the cube were constrained to move within their plane and a vertical displacement of 10 units was applied to the nodes along the cube's upper face. To model nearly incompressible behavior, an elastic modulus, E, of $E=200$ GPa and a Poisson's ratio, υ, of 0.4999 were defined for the cube.

Results of equivalent strain and hydrostatic pressures (Figs. 3 and 4) were determined for the new element and for a constant pressure quadratic tetrahedral element and a hexahedral element with mixed u/p and B-bar formulation. Both of these elements are known to pass the strict BB condition and perform well in the incompressibility limit. As shown in the figures, the performance of the stabilized low-order tetrahedral surpasses the quadratic tetrahedral element with constant pressure since the quadratic element diverges at 70% of the total deformation and shows non-homogeneous deformation behavior. The strains and the hydrostatic pressure obtained using the stabilized four-node tetrahedron are identical with the corresponding values obtained for the hexahedral element with mixed u/p and B-bar formulation. Such a finding is important as it indicates that the proposed formulation is capable of representing the homogeneous deformation state in extremely large deformations at the incompressibility limit without locking.

3.2. Upsetting of a billet

To further assess the performance of the new mixed-enhanced deformation tetrahedral element under conditions of elasto-plastic finite deformation, a billet upsetting process was analyzed. In the upsetting problem, the billet was modeled as a block with dimensions $10 \times 30 \times 1$ mm that was subject to a distributed displacement load applied over one-third of its top cross-sectional area (see Fig. 5). The overall objective of the forming process being modeled was to achieve a 65% compression of the height of the billet. In the simulation, the material properties of the billet were given the following values:

elastic modulus(E) : 200 GPa, Poison′s ratio(ν) : 0.3,

yield stress(σ_y) : 250 MPa, tangent modulus(E_T) : 1.0 GPa.

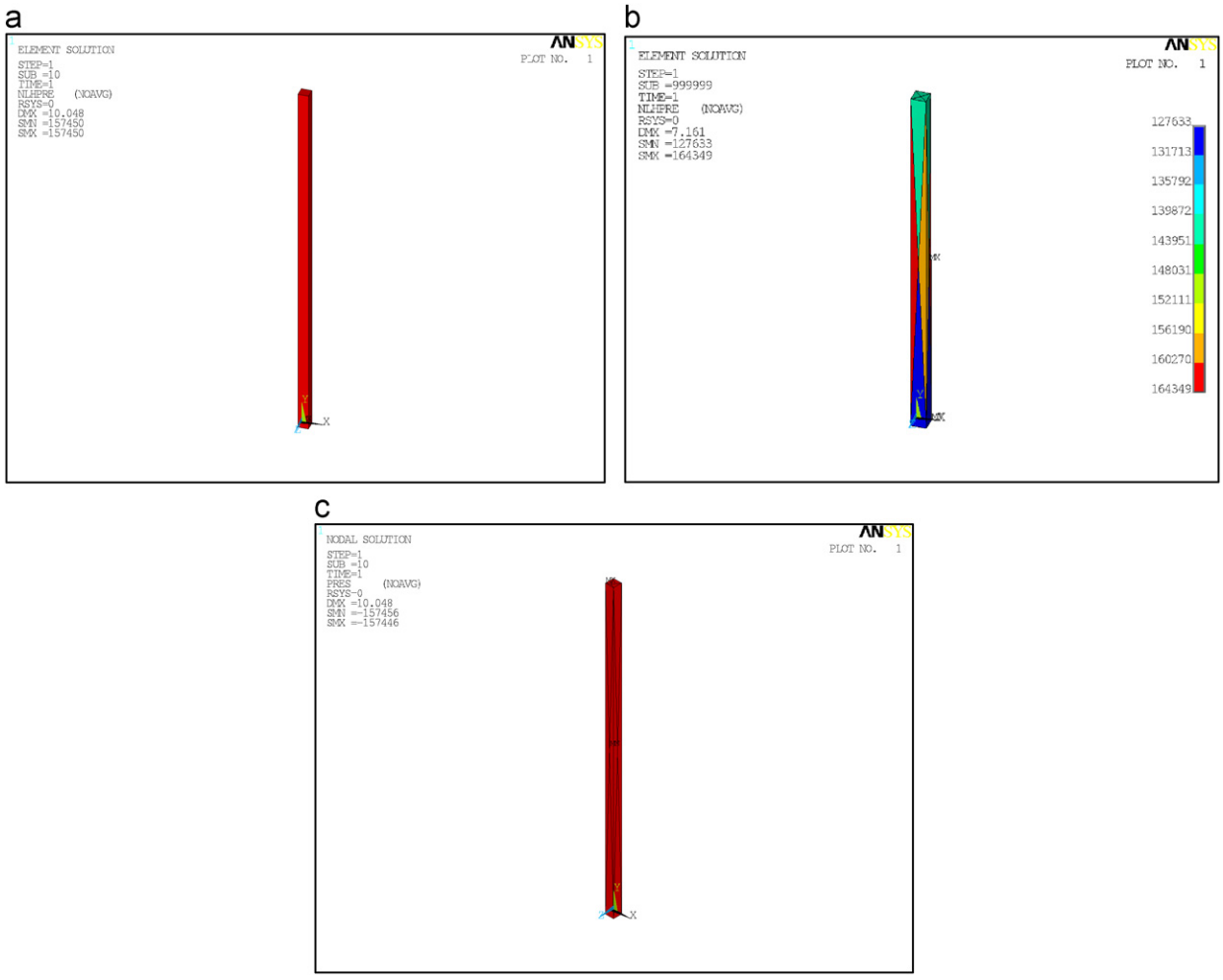

Fig. 4. Homogeneous deformation test: hydrostatic pressure. (a) Mixed u/p hexahedral, (b) constant pressure 10 node tetrahedral, (c) stabilized mixed u/p four-node tetrahedral.

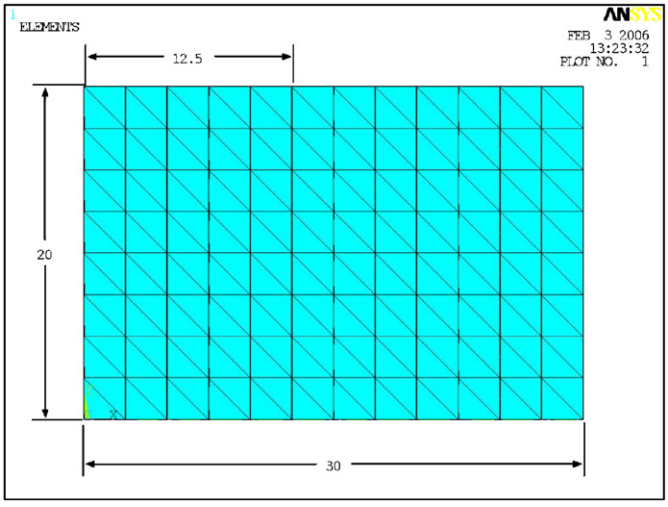

Fig. 5. Geometry and BC's of the upsetting model.

The finite element model used in this simulation has a structured mesh that permits direct comparison with a hexahedral element mesh. Using the model, results were compared with: (1) standard and mixed u/p formulation without stabilization, (2) quadratic constant and linear pressure tetrahedral meshes and (3) mixed u/p hexahedral mesh. Out of the three different element types used for comparison, the quadratic constant pressure tetrahedral and the mixed u/p hexahedral elements are known to pass the BB condition while the popular linear pressure quadratic tetrahedron fails the BB condition. Figs. 6 and 7 contain contour plots of the equivalent stress of the deformed billet and principal stress in the second direction. As shown in the figures, good agreement was obtained between the predicted deformation and stress results of the linear pressure quadratic tetrahedral, the hexahedral elements and our new formulation. The constant pressure quadratic tetrahedral model diverged at 51% of total deformation and therefore could not be used for comparison. Examining the contour plots of all three formulations for the four-node tetrahedral element, the stabilized formulation is the only one that predicts the correct deformed shape and displacement. Looking at the maximum displacement and principal stresses, the new element is closer to the mixed u/p hexahedral element than to the quadratic linear pressure

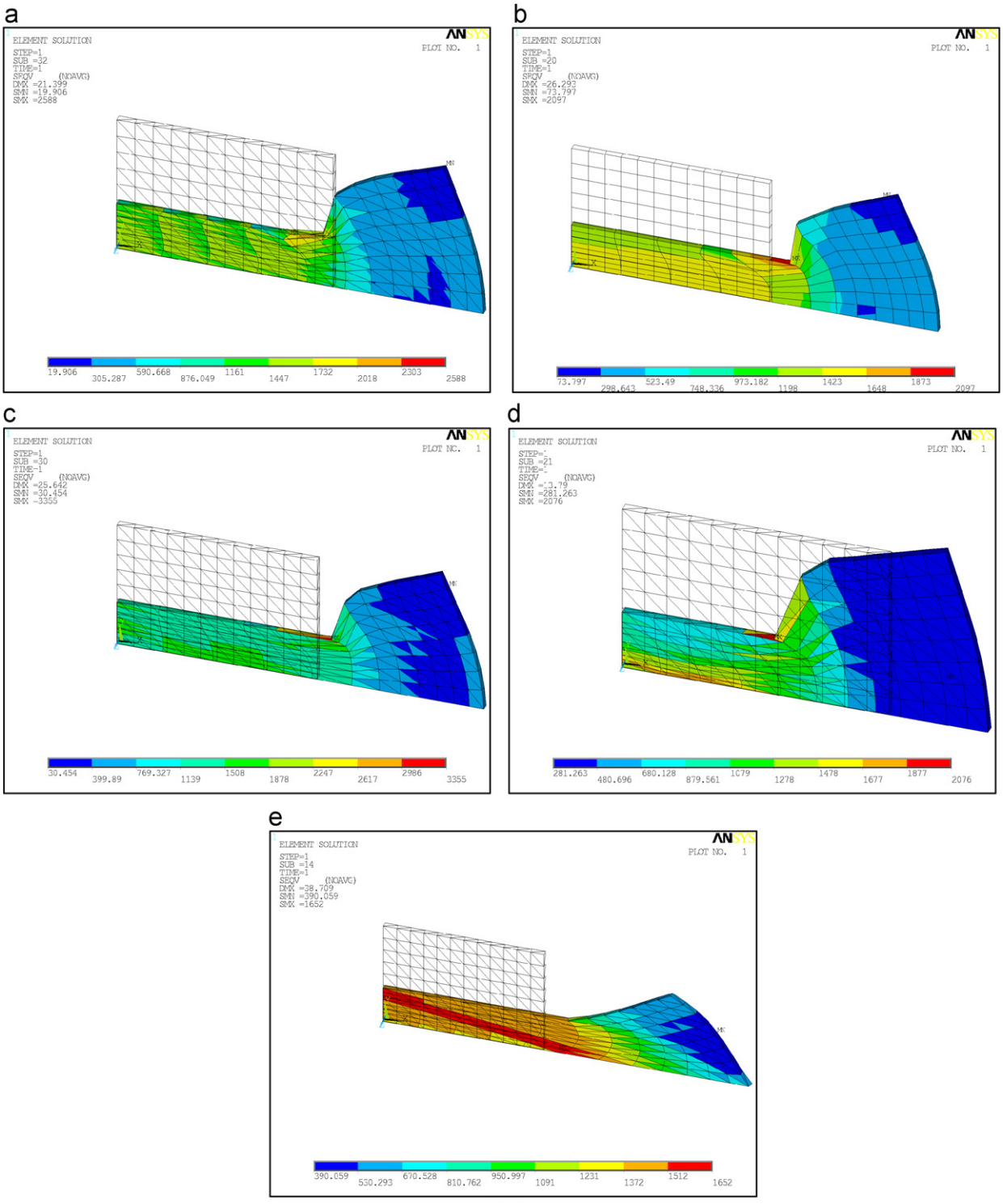

Fig. 6. Upsetting of a billet: equivalent stress. (a) Linear pressure 10 node tetrahedral, (b) mixed u/p hexahedral, (c) stabilized mixed u/p four-node tetrahedral, (d) mixed u/p four-node tetrahedral, (e) pure displacement four-node tetrahedral.

element which clearly shows volumetric locking due to the high principal stresses. The mixed u/p formulation without stabilization predicts fairly accurate values for the equivalent stress but dramatically underestimates the displacements. The deformation of the mixed u/p formulation also incorrectly predicts an upward direction of plastic flow. The pure displacement formulation shows evidence of locking by the appearance of classical checkerboard pattern and high values of principal stress. The stabilization effect of the mixed-enhanced deformation formulation is obvious from the plots of the second principal stress

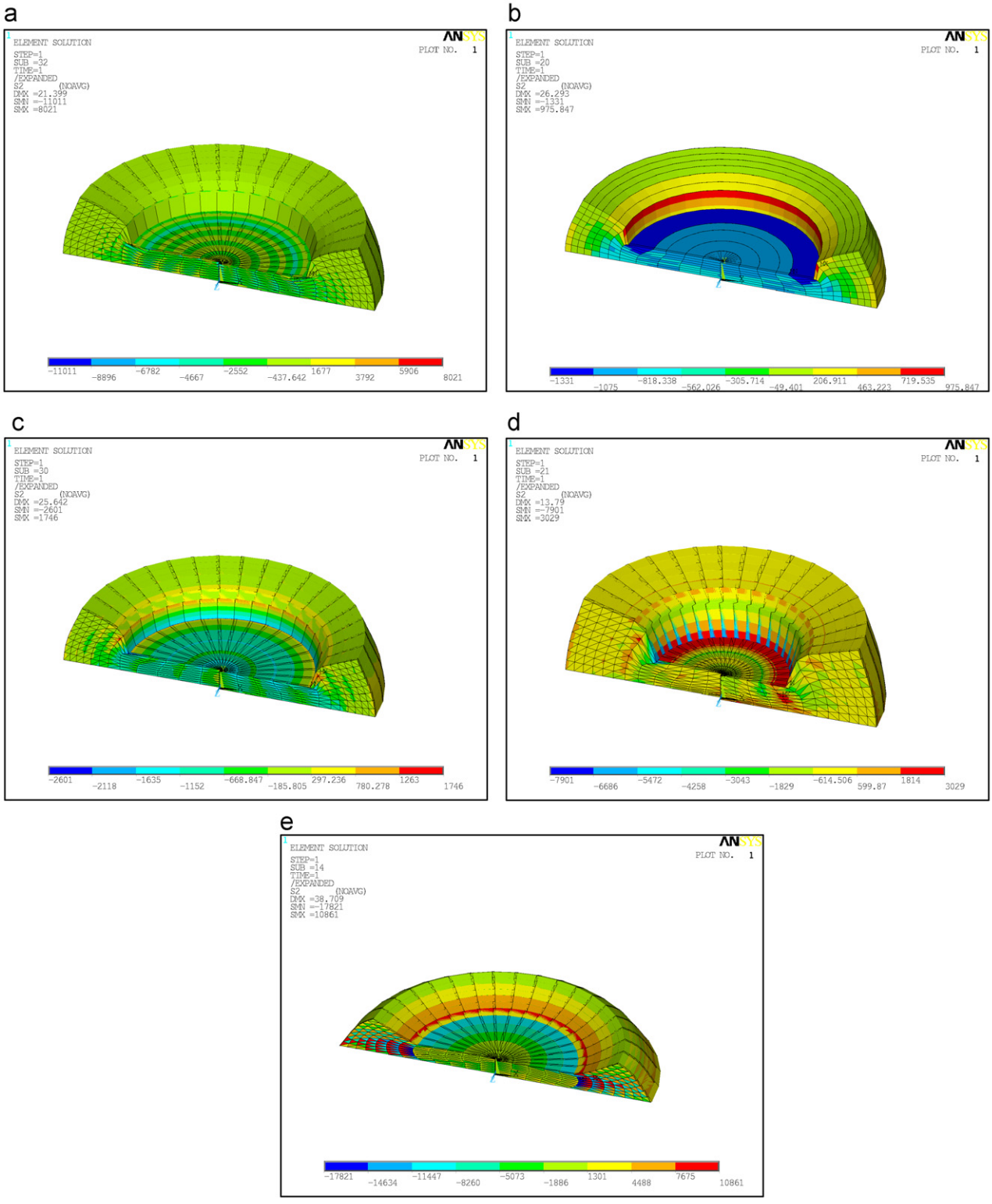

Fig. 7. Upsetting of a billet: principal stress in second direction. (a) Linear pressure 10 node tetrahedral, (b) mixed u/p hexahedral, (c) stabilized mixed u/p four-node tetrahedral, (d) mixed u/p four-node tetrahedral, (e) pure displacement four-node tetrahedral.

which show a smooth distribution in contrast to the polluted distribution of stresses obtained with the mixed formulation without stabilization.

Even though the results are improved over the other available formulations for tetrahedral elements, there are still some differences between the new tetrahedral element formulation results

and those obtained with a hexahedral element. The difference in the predicted results relates to the deformation of the billet around the punch corner where the tetrahedral model predicts a smaller slope between the punch face and the free surface. In this area, the mesh is distorted for the tetrahedral elements which lead to compressive stresses that are much higher than the hexahedral elements. The sharp corner in the model represents a singularity and therefore it is expected that the tetrahedral and hexahedral elements would predict different values in this area.

Overall it can be concluded that the stabilized mixed u/p lower-order tetrahedral element provides better accuracy than the higher-order tetrahedral with linearly distributed pressure and better convergence than the constant pressure higher-order tetrahedral element.

4. Conclusions

The main goal of the present paper was to develop a robust and accurate lower-order solid tetrahedral element that exhibits significantly better performance than the existing elements. This work was motivated by the absence of a tetrahedral element that was capable of solving general large deformation problems under incompressible conditions that can incorporate a wide range of nonlinear materials. After describing the theoretical formulation of the element, two numerical examples were used to demonstrate the robustness, accuracy and improved performance of the proposed formulation in quasi and fully incompressible problems that involved large deformation. The upsetting problem showed that the stabilized formulation brings consistent improvement over the mixed u/p without stabilization and the pure displacement formulations. This observation was noted by the more accurate stress and displacements distribution when compared to quadratic element. The importance of the new lower-order tetrahedral element lies within its ability to provide large deformation analysis capabilities for problems where the automatic generation of hexahedral elements is not possible, especially when rezoning procedures need to be applied. Such technology is an important step in the advancing simulation of the metal forming and other complex engineering processes.

References

[1] T. Belytschko, W.K. Liu, B. Moran, Nonlinear Finite Elements for Continua and Structures, Wiley, New York, 2000, pp. 451–507.
[2] I. Babuška, Error bounds for finite element methods, Numer. Math. 16 (1971) 322–333.
[3] M. Cervera, M. Chiumenti, Q. Valverde, C.A. de Saracibar, Mixed linear/linear simplicial elements for incompressible elasticity and plasticity, Comput. Methods Appl. Mech. Eng. 192 (2003) 5249–5263.
[4] M. Chiumenti, Q. Valverde, C. Agelet de Saracibar, M. Cervera, A stabilized formulation for incompressible elasticity using linear displacement and pressure interpolations, Comput. Methods Appl. Mech. Eng. 191 (2002) 5253–5264.
[5] E. Oñate, J. Rojek, R.L. Taylor, O.C. Zienkiewicz, Finite calculus formulation for incompressible solids using linear triangles and tetrahedra, Int. J. Numer. Methods Eng. 59 (2004) 1473–1500.
[6] M. Chiumenti, Q. Valverde, C. Agelet de Saracibar, M. Cervera, A stabilized formulation for incompressible plasticity using linear triangles and tetrahedra, Int. J. Plast. 20 (2004) 1487–1504.
[7] M. Pastor, M. Quecedo, O.C. Zienkiewicz, A mixed displacement–pressure formulation for numerical analysis of plastic failure, Comput. Struct. 62 (1) (1997) 13–23.
[8] M. Quecedo, M. Pastor, O.C. Zienkiewicz, Enhanced linear triangle for plasticity problems in J_2 solids, Comput. Methods Appl. Mech. Eng. 188 (2000) 145–163.
[9] O. Klaas, A. Maniatty, M.S. Shephard, A stabilized mixed finite element method for finite elasticity. Formulation for linear displacement and pressure interpolation, Comput. Methods Appl. Mech. Eng. 180 (1999) 65–79.
[10] R.L. Taylor, A mixed-enhanced formulation for tetrahedral finite elements, Int. J. Numer. Methods Eng. 47 (2000) 205–227.
[11] D.N. Arnold, F. Brezzi, M. Fortin, A stable finite element for the Stokes equations, Calcolo 21 (1984) 337–344.
[12] J. Bonet, A. Burton, A simple average nodal pressure tetrahedral element for incompressible and nearly incompressible dynamic explicit applications, Commun. Numer. Methods Eng. 14 (1998) 437–449.
[13] F. Brezzi, J. Pitkäranta, On the stabilization of finite element approximations of the Stokes problem, in: W. Hackbusch (Ed.), Efficient Solution of Elliptic Problems, Notes on Numerical Fluid Mechanics, vol. 10, Vieweg, Wiesbaden, 1984.
[14] O.C. Zienkiewicz, R. Taylor, The Finite Element Method, The Basis, vol. 1, fifth ed., McGraw-Hill, London, 2000.
[15] T.J.R. Hughes, Multiscale phenomena: Green's functions, the Dirichlet-to-Neumann formulation, subgrid scale models, bubbles and the origins of stabilized methods, Comput. Methods Appl. Mech. Eng. 127 (1995) 387–401.
[16] R. Codina, Stabilized finite element approximation of transient incompressible flows using orthogonal subscales, Comput. Methods Appl. Mech. Eng. 191 (2002) 4295–4321.
[17] E. Oñate, Multiscale computational analysis in mechanics using finite calculus: an introduction, Comput. Methods Appl. Mech. Eng. 192 (2003) 3043–3059.
[18] R. Pierre, Simple C^0 approximations for the computation of incompressible flows, Comput. Methods Appl. Mech. Eng. 68 (1988) 205–227.
[19] T. Sussman, K.-J. Bathe, A finite element formulation for nonlinear incompressible elastic and inelastic analysis, Comput. Struct. 26 (1987) 357–409.
[20] J.D. Lee, Finite element procedures for large strain elastic–plastic theories, Comput. Struct. 28 (1988) 395–406.
[21] M.S. Gadala, J. Wang, Simulation of metal forming processes with finite element methods, Int. J. Numer. Methods Eng. 44 (1999) 1397–1428.
[22] K.-J. Bathe, Finite Element Procedures, Prentice-Hall, Upper Saddle River, NJ, 1996.
[23] R.M. McMeeking, J. Rice, Finite-element formulations for problems of large elastic–plastic deformation, Int. J. Solids Struct. 11 (1975) 601–616.
[24] J.C. Simo, F. Armero, Improved versions of assumed enhanced strain tri-linear elements for 3D finite deformation problems, Comput. Methods Appl. Mech. Eng. 110 (1993) 359–386.
[25] T.J. R Hughes, J. Winget, Finite rotations effects in numerical integration of rate constitutive equations arising in large-deformation analysis, Short Commun. (1980) 1862–1867.